

Raman Spectroscopy of Polycrystalline α - MnSe

A. Milutinović, Z. V. Popović, N. Tomić and S. Dević

Center for Solid State Physics and New Materials,
Institute of Physics, Belgrade, Serbia and Montenegro

Keywords: Phonons, Photoluminescence, Raman Spectroscopy, Spin Excitation

ABSTRACT

Polycrystalline α -MnSe samples are investigated by Raman and photoluminescence spectroscopy. We assigned the first and the second order phonons in Raman spectra by a help of rigid ion model calculations. Several modes connected with spin system, whose width and frequencies depend on temperature, are assigned, too. Photoluminescence in α -MnSe shows a step-like shift of emission bands below T_N , in correlation with the antiferromagnetic spin-ordering in this material.

1. INTRODUCTION

Manganese oxides and chalcogenides, their alloys and superlattices have been of great interest for years because of the relevance of their magneto-optical and transport properties to applications such as infrared detectors, solar cells and spintronic devices in recent future [1-4]. In the case of MnSe, the dominant crystal structure in both the paramagnetic and the antiferromagnetic (AFM) phase is cubic, of NaCl type (α -phase), whereas the second phase with hexagonal NiAs crystal structure arises at about 190 K (during cooling). The "NiAs" structure of MnSe consists of ferromagnetic sheets, stacked antiferromagnetically perpendicular to the c -axis. The number and the size of "NiAs" bands increase with decreasing of temperature and, according to Ref. [3], may occupy 15-38 % of crystal volume. On warming, the "NiAs" modification converts to the cubic form and completely vanishes at 300 K staying magnetic up to this temperature. Because of that, some magnetic and neutron diffraction measurements were contradictory interpreted [6-10]. The cubic form itself exhibits AFM-II [5] spin ordering, with the Néel temperature of 122 K [3], or between 130 and 250 K, due to thermal hysteresis and sample history effects, as reported by other authors [6-8]. In our previous paper [11], we found $T_N = 90$ K for α -MnSe with neglecting content of "NiAs"- phase. The cubic form can be fixed by adding 10% magnesium [12]. MnSe can also be stabilized artificially in the zinc blende (β -phase) structure by epitaxial growth or by alloying with II-VI semiconductors [5].

Optical phonons of α -MnSe were investigated by far-infrared reflectivity [13] at room and liquid nitrogen temperature without any evidence of the presence of the "NiAs"-phase in α -MnSe. Optical phonons were Raman inactive in the paramagnetic phase of the α -MnSe. There is no data about Raman scattering by optical phonons in the antiferromagnetic phase of α -MnSe. In our previous work [11], we found the one-magnon mode at 18 cm^{-1} in the Raman spectra.

In the present work, we investigate polycrystalline α -MnSe samples by Raman and photoluminescence spectroscopy. We calculate the phonon dispersion relation for rock salt α -MnSe crystals using the rigid ion model (RIM). Based on that simple model, we assign the first and the second order phonon modes in Raman spectra of α -MnSe. Several modes show dramatic mode width and frequency change by lowering the temperature. We assigned them as spin-related. We

also investigate photoluminescence in α -MnSe. A step-like shift of emission bands below T_N demonstrates its correlation with the AFM spin-ordering in this material.

2. EXPERIMENT

Polycrystalline α -MnSe samples were made by a sintering technique. Details of sample preparation were published in Ref. [11]. The quality of α -MnSe samples was checked by X-ray diffractometry. No traces of starting elements or impurity phases confirm a good quality of the samples. Raman measurements were performed in the back scattering geometry using a Dilor X-Y 800 spectrometer equipped with a CCD detector. In order to avoid the sample heating we used a line focus. Photoluminescence measurements were done using a Joben-Yvon U1000 monochromator with a standard photon-counting system. Low-temperature spectra were recorded using Leybold closed-cycle helium cryostat.

3. RESULTS AND DISCUSSION

As we have already mentioned, α -MnSe has a NaCl-type structure with O_h symmetry and only one infrared (IR) active mode of F_{1u} symmetry. Hexagonal “NiAs” modification, with symmetry $P6_3mc$ (which may arise under 190 K) has $1E_{2g}$ Raman active and $A_{2u}+E_{1u}$ IR active modes. In both modifications Mn^{2+} ions are in the same fcc-like (octahedral) environment, but in the “NiAs” modification, the surrounding of Se is hcp-like. We believe that this one Raman active mode, E_{2g} , should be seen in the low-temperature spectra if the amount of “NiAs” phase becomes significant.

Raman spectra of α -MnSe were measured in the spectral range between 70 and 800 cm^{-1} at temperatures between 6 and 300 K. The rock salt structure has no Raman active modes, but there

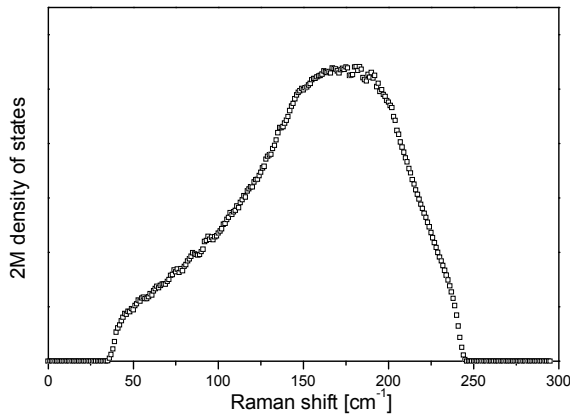


Fig. 1: Density of states for two-magnon scattering process

are three irreducible components A_{1g} , T_{2g} and E_g of a second-rank tensor. All combinations of modes can be observed in our unpolarized measurements on the polycrystalline samples, i.e., summation bands, difference bands (at low temperatures) and overtones [14]. Crystal imperfections led to the relaxation of selection rules and modes from the center of Brillouin zone (BZ) can be observed, too. Modes clearly seen at low temperatures are also seen in the high temperature range except a few very weak features that could not be resolved. The frequencies of these weak modes at 155 and 175 cm^{-1} seem to be temperature dependent, but the quality of spectra did not allow a quantitative analysis. Mode at 155 cm^{-1} could be a combination of TO mode and acoustic one-magnon: $\omega_{TO}(\Gamma) + \omega_{1Mac} = 138 \text{ cm}^{-1} + 18 \text{ cm}^{-1} = 156 \text{ cm}^{-1}$, and the mode at 175 cm^{-1} is an acoustic two-magnon excitation. In our previous paper [11], we estimated the exchange energies of $J_{1(NN)} = 3.375 \text{ cm}^{-1}$, $J_{2(NNN)} = 5.625 \text{ cm}^{-1}$, and the anisotropy parameter $D_1 = 0.236 \text{ cm}^{-1}$. Based on supposed model and one-magnon dispersion relations, $\omega_{1M}(\mathbf{k})$, we obtained the density of states for two-magnon scattering process, Fig.1. The two-magnon Raman intensity (for low temperatures) is proportional to the imaginary part of the Green function and can be evaluated by a standard procedure [15] following the relation:

$$I_{2M} \propto \text{Im} \left[\frac{1}{N} \sum_{\mathbf{k}} \frac{\Phi(\bar{\mathbf{k}})}{\omega^2 - 4\omega_{1M}^2(\bar{\mathbf{k}})} \right] = \frac{\pi}{4N} \sum_{\mathbf{k}} \frac{\Phi(\bar{\mathbf{k}})}{\omega_{1M}(\bar{\mathbf{k}})} \delta(\omega - 2\omega_{1M}(\bar{\mathbf{k}}))$$

$\Phi(k)$ is the symmetry factor, which for cubic structure does not affect the shape of function $I_{2M}(\omega)$. Summation was done for k_x, k_y, k_z in the interval 0 to $\pi/2a$ (magnetic elementary cell is twice as paramagnetic cell), channel for wave vector was 1cm^{-1} , like the experimental error. As it is shown in Fig. 1, the maximum of density is obtained at 175cm^{-1} .

The deconvolution of Raman spectra shows that the broadening of LO mode (237cm^{-1}) from the center of BZ is temperature dependent (see Fig. 2). With increasing temperature, the mode width decreases. At temperatures above 105 K this mode becomes more pronounced. As can be seen from the inset of Fig. 2, the LO mode width starts to change when the temperature is close to $T_N = 90\text{K}$.

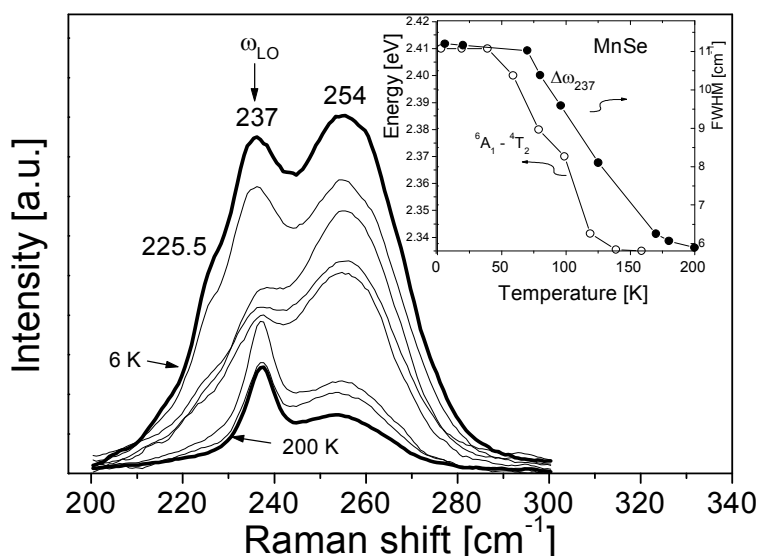


Fig. 2. The change of the LO-mode intensity and broadening with temperature. In the inset: The temperature dependences of the LO-mode width (FWHM) and ${}^6A_1-{}^4T_2$ excitation energy, Ref.[21].

${}^6A_1 \rightarrow {}^4T_2$ transition and our Raman spectra become resonantly enhanced at lower temperature. Since energy change of ${}^6A_1 \rightarrow {}^4T_2$ transition is related to the spin ordering, spin dynamics leave a fingerprint to the intensity and line width of all optical modes, as it is illustrated in Figs 2 and 3.

The modes, that appear at frequencies 360 and 459cm^{-1} , measured at 6K , show strong temperature dependence, Fig. 3. These modes are in connection with the spin excitation, too. The both of them can be two-magnon scattering processes related. Weaker mode at 360cm^{-1} is a second harmonic of two-magnon acoustic, and the mode at 459cm^{-1} is optical two-magnon excitation. Because isomorphous crystals MnO and MnS have the values of exchange energies, dipolar anisotropy and acoustic magnon [16] in the same range as α -MnSe, the optical magnon branches of α -MnSe could have energy like optical magnon branches of these crystals.

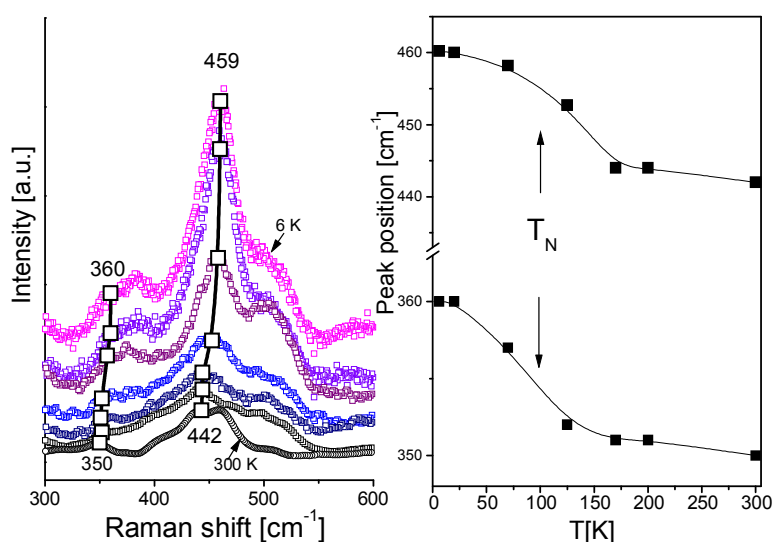


Fig. 3: Temperature dependence of two-magnon excitations: at 360cm^{-1} is the second harmonic of acoustic two-magnon excitation; at 459cm^{-1} is a optical two-magnon excitation (full lines are guides for the eye)

A dramatic change in 237cm^{-1} mode intensity and its broadening by lowering of temperature is most probable a resonance effect related. In the inset of Fig. 2 the energy versus temperature dependence of ${}^6A_1 \rightarrow {}^4T_2$ transition in MnSe is shown, Ref. [21]. As it can be seen from the inset, the energy of this transition changes from 2.335eV (at 160K) to 2.41eV at temperatures lower than 60K . Raman spectra were measured with 514.5nm (2.41eV) line of an argon laser. By lowering the temperature, the laser energy fits the energy value of

In order to assign the first and the second order modes in Raman spectra we calculated the phonon dispersion for α -MnSe using the rigid ion model (RIM) [17]. In the calculation, we used the following values of input parameters: $r_0 = a/2 = 2.7115 \text{ \AA}$, $A = 11.55Z'^2$, $B = -1.165Z'^2$, effective charge $Z' = 1.3465$, $\omega_{\text{TO}}(\Gamma) = 137 \text{ cm}^{-1}$, $\omega_{\text{LO}}(\Gamma) = 237 \text{ cm}^{-1}$, $\epsilon_0 = 25$, $\epsilon_\infty = 7.3$ (parameters ϵ_0 and ϵ_∞ are taken from our far-infrared reflectivity measurements).

Effective charge Z' is calculated by comparing the values of compressibility obtained from the model and those from the optical measurements [17, 18] and this value is used in a model. Calculated elastic constants in units of $10^{-12} \text{ Dyn/cm}^2$ are: $c_{11}=1.3614$; $c_{12}=0.2698$; $c_{44}=0.2693$. On the basis of this simple model we offered a possible explanation of the origin of weak modes in Raman spectra. The positions of the first order and the secondary modes in Raman spectra are compared with the calculated ones, Table 1. Modes pointed out with asterisk, which are connected with spin excitation, are given in Table 1, too.

Photoluminescence spectra of α -MnSe (excited by 514.5 nm Ar-ion laser line) in the energy range of 1.4 to 2.4 eV are presented in Fig.4. The photoluminescence bands could be excited via energy transfer by the “d-d” transitions from the ${}^6A_{1,1g}$ ground state into various excited states of the Mn^{2+} ions. These “d-d” transitions are not of pure “d” origin but mixing of Mn $3d^5$ and Se $4p^4$ states [19, 20].

At low temperatures, an energy band at about 1.51 eV has strong intensity and partially masks a luminescence band at 1.70 eV. This band at 1.51 eV is caused by an energy transfer mechanism from excited Mn^{2+} ions via Mn sublattice to Mn ions in a disturbed environment [21]. At about 2.15 eV, an emission due to direct internal ${}^4T_{1g} \rightarrow {}^6A_1$ transition is observed.

Step-like shift in photoluminescence peak positions below the Néel temperature, T_N , demonstrates the correlation

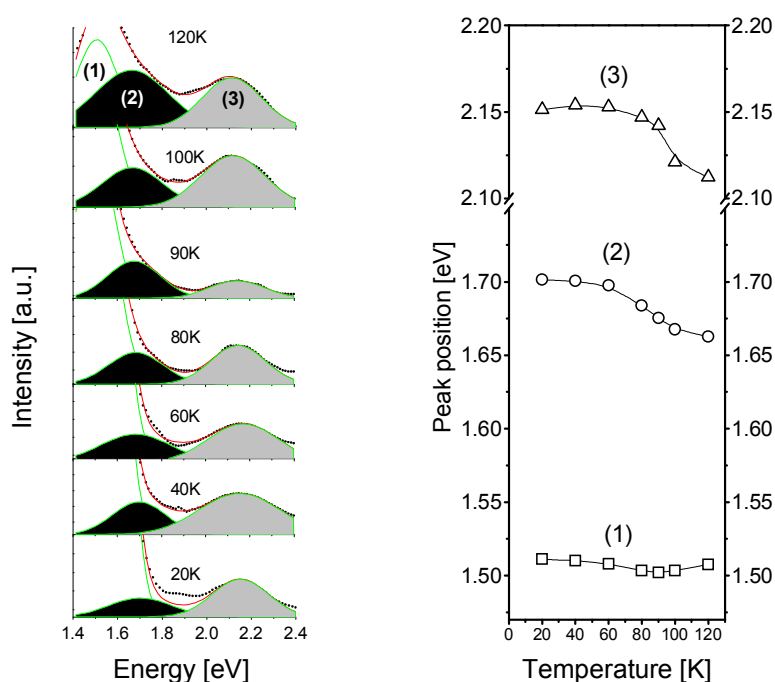


Fig. 4: Luminescence spectra of α -MnSe and the temperature dependence of peak position

Table 1

Assignment of Raman peaks in α -MnSe

Assignment	Calculated values [cm^{-1}]	Measured values [cm^{-1}]
TA(X)	76.7	73
LO-TO(X)	83.3	84
TA(L)	87.9	91
LO-TO(Γ)	99	99
TO(L)	105.3	105
TO(X)	113.6	115
LA (X)	132.9	128
TO(Γ)	137	138
TO+1M_{ac}(Γ)	*155 *	155
2M_{ac}	*175*	174,184
TO+TA(X)	190.3	192
TO+TA(L)	193.2	200
LA+TA(X)	209.6	215
2TO(X)	227.2	224
LO (Γ)	234.5	237
TO+LA (X)	246.5	251
TO+LA (L)	257.5	260
2(2M_{ac})	*350*	360
2(TO+TA)(X)	380.6	383
2M_{opt.}	*?*	459
2(TO+LA)(X)	493	502
2(TO+LA)(L)	515	520

between the antiferromagnetic spin ordering and the energies of Mn^{2+} internal transitions. Different relaxation energies for the ground and excited Mn^{2+} states are responsible for this behavior. (The maximum total shift between T_N and 0K is observed for ${}^4T_{2g} \rightarrow {}^6A_1$ in MnS [22]. In α -MnSe this excitation band is at 2.41 eV [21] and we could not observe it in our experiment.)

In the case of NaCl structure, the anions lie on the edges of the cubic fcc cell between the second-nearest magnetic neighbors. As a result, the next-nearest-neighbor (NNN) interaction (d-p-d superexchange interaction) is

usually stronger than the nearest-neighbor (NN) interaction. The magnetic anisotropy energy is expected to be mainly of dipolar origin, and very small compared to the isotropic exchange energy. In the first approximation, energy relaxation of Mn^{2+} ion can be described on the basis of the isotropic part of Hamiltonian neglecting the nearest neighbor interaction. Energy difference between the ground and the excited state, in this approximation is given by:

$$\Delta E = -6(J_{2g}S^2 - J_{2exc}SS'),$$

where $J_{2g(exc)}$ is NNN exchange interaction for ground (excited) state; spin $S=5/2$ for $T=0$ K, $S=3/2$ [19] for excited states; 6-number of next nearest neighbors. Value of $J_{2g} = 5.625 \text{ cm}^{-1}$ corresponds to the ground state, $\Delta E = 0.0398 \text{ eV}$ is the measured value of shift for the second luminescence band and we calculate $J_{2exc} = 4.8911 \text{ cm}^{-1}$. Shift of 2.15 eV band, was $\Delta E = 0.0417 \text{ eV}$ giving exchange interaction parameter $J_{2exc} = 5.5721 \text{ cm}^{-1}$. It seems that J_2 stay unperturbed and that the energy shift of corresponding band is mainly caused by spin difference.

4. CONCLUSIONS

We investigated polycrystalline α -MnSe samples by Raman and photoluminescence spectroscopy. The first and the second order phonons in Raman spectra are assigned by a help of rigid ion model calculations. Some modes show a dramatic change of the mode width and frequencies by temperature decrease. We assigned them as spin-related. The density of magnon states is calculated. The calculated value of the acoustic two-magnon excitation is fully in agreement with the observed second harmonic of two-magnon peak in Raman spectra. Photoluminescence in α -MnSe shows a step-like shift of emission bands below T_N , in correlation with the antiferromagnetic spin-ordering in this material. The total energy shift of photoluminescence bands is mainly caused by spin difference between ground, 6A_1 , and excited state, ${}^4T_{1g}$.

REFERENCES

- [1] S. A. Wolf, D. D. Awschalom, R. A. Buhrman, J. M. Daughton, S. Molnár, M. L. Roukes, A. Y. Chtchelkanova, and D. M. Treger, *Science* **294**, 1488 (2001).
- [2] D. R. Huffman and R. L. Wild, *Phys. Rev.* **118**, 526 (1966).
- [3] R. J. Pollard, V. H. McCann, and J. B. Ward, *J. Phys. C* **16**, 345 (1983).
- [4] K. Ozawa, S. Anzai, and Y. Hamaguchi, *Phys. Lett.* **20**, 132 (1966).
- [5] P. Klosowski, T. M. Giebultowicz, J. J. Rhyne, N. Samarth, H. Luo, and J. Furdyna, *J. Appl. Phys.* **69**, 6109 (1991).
- [6] R. Lindsay, *Phys. Rev.* **84**, 569 (1951).
- [7] J. J. Banewicz, R. F. Haidelberg, and A. H. Luxem, *J. Phys. Chem.* **65**, 615 (1961)
- [8] P. W. Anderson, *Phys. Rev.* **79**, 705 (1950)
- [9] A. F. Andersen and H. Rotterud, *Acta Crystallogr., Sect. A: Cryst. Phys., Diffr., Theor. Gen. Crystallogr.* **25**, S250 (1969).
- [10] A. J. Jacobson and B. E. F. Fender, *J. Chem. Phys.* **52**, 4563 (1970).
- [11] A. Milutinovic, N. Tomic, S. Devic, P. Milutinovic, and Z. V. Popovic, *Phys. Rev. B*, **66**, 012302 (2002).
- [12] H. van der Heide, J. P. Sanchez, and C. F. van Bruggen, *J. Magn. & Magn. Mater.* **15-18**, 1157 (1980).
- [13] D. L. Decker and R. L. Wild, *Phys. Rev. B* **4**, 3425 (1971).
- [14] K. H. Rieder, B. A. Weinstein, M. Cardona, and H. Bilz, *Phys. Rev. B* **10**, 4780 (1973).
- [15] T. Holstein and H. Primakoff, *Phys. Rev.* **58**, 1098 (1940).
- [16] H-h. Chou and H. Y. Fan, *Phys. Rev. B*, **13**, 3924 (1976).

- [17] M. Born and K. Huang : Dynamical theory of crystal lattices, Oxford, Clarendon press, 1954.
- [18] A. D. B. Woods, W. Cochran, and B. N. Brockhouse, Phys. Rev. **119**, 980 (1960).
- [19] H. Sato, T. Mihara, A. Furuta, M. Tamura, K. Mimura, N. Happono, M. Taniguchi, and Y. Ueda , Phys. Rev. B **56**, 7222 (1997).
- [20] S.-H. Wei and A. Zunger, J. Cryst. Growth **86**, 1(1988).
- [21] W. Heimbrod, O. Goede, I. Tschentscher, V. Weinhold, A. Klimakow, U. Pohl, K. Jacobs, and N. Hoffmann, Physica B **185**(1993)357.
- [22] W. Heimbrod, C. Benecke, O. Goede, and H.-E. Gumlich, J. Cryst. Growth **101**, 911 (1990).